BIOCHEMISTRY
including biophysical chemistry & molecular biology

Article

pubs.acs.org/biochemistry

Structures of KcsA in Complex with Symmetrical Quaternary Ammonium Compounds Reveal a Hydrophobic Binding Site

Michael J. Lenaeus,[†] Dylan Burdette,[‡] Tobias Wagner,[†] Pamela J. Focia,[†] and Adrian Gross*[,†,‡]

[†]Department of Molecular Pharmacology and Biological Chemistry, Northwestern University Medical School, 303 East Chicago Avenue, Chicago, Illinois 60611, United States

[‡]Department of Biochemistry and Molecular Biology, Rosalind Franklin University of Medicine and Science, 3333 Green Bay Road, North Chicago, Illinois 60064, United States

ABSTRACT: Potassium channels allow for the passive movement of potassium ions across the cell membrane and are instrumental in controlling the membrane potential in all cell types. Quaternary ammonium (QA) compounds block potassium channels and have long been used to study the functional and structural properties of these channels. Here we describe the interaction between three symmetrical hydrophobic QAs and the prokaryotic potassium channel KcsA. The structures demonstrate the presence of a hydrophobic pocket between the inner helices of KcsA and provide insight into the binding site and blocking mechanism of hydrophobic QAs. The structures also reveal a structurally hidden pathway between the central cavity and the outside membrane environment reminiscent of the lateral fenestration observed in sodium channels that can be accessed through small conformational changes in the pore wall. We propose that the hydrophobic binding pocket stabilizes the alkyl chains of long-chain QA molecules and may play a key role in hydrophobic drug binding in general.

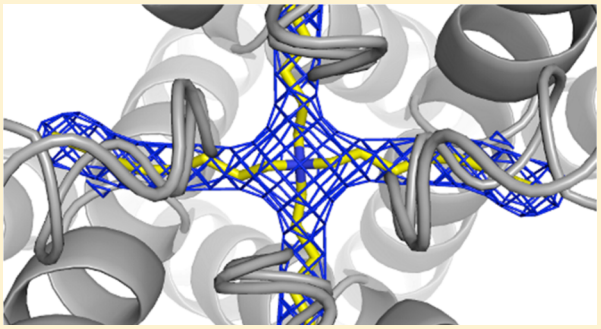

Quaternary ammonium (QA) compounds have long been used in the study of potassium channels and have greatly contributed to our understanding of their structural and functional properties. QA compounds compete with potassium at ion binding sites in the channel and impede potassium flow because they are unable to permeate across the narrow selectivity filter. Tetraethylammonium (TEA), the most widely studied QA, can bind to potassium channels on both sides of the membrane with comparable affinity.[1,2] Hydrophobic QAs, on the other hand, show a marked preference for internal binding. Indeed, early work by Armstrong on the squid giant axon showed that the binding affinity of long-chain TEA analogues (Figure 1A) increased with increasing alkyl-chain length, suggesting that hydrophobic interactions were important for the stabilization of QA compounds on the internal side of the channel.[3] In this series of landmark experiments, Armstrong showed that internally applied long-chain QAs act as open channel blockers that can be trapped in the pore under favorable conditions and that the binding of these ligands can increase the rate of slow inactivation in the squid giant axon potassium channel.[3−5] These concepts were also demonstrated and extended by Yellen and co-workers on the cloned Shaker potassium channel,[6−8] leading to a precrystallographic consensus view of the QA−channel interaction that can be summarized as follows. First, QAs and other related drugs bind at potassium binding sites between the selectivity filter and the gate and are further stabilized through favorable hydrophobic interactions with the cavity wall. Second, QAs can be trapped within the channel if there is enough room in the pathway to accommodate them in both the open and closed states.[3] Trapping can be facilitated through a reduction in the size of pathway-exposed residues,[9,10] and conversely, trapping can be prevented if the drug interferes with the closing of the intracellular gate through a "foot in the door" mechanism.[3,6,9,11] Third, QAs promote slow inactivation by emptying the selectivity filter of potassium. Higher-affinity blockers have longer dwell times at the binding site, leading to increased loss of potassium to the external solution and enhanced inactivation.[3,7,8]

The ability to determine atomic structures of potassium channels has led to further study of the QA−channel interaction. Crystallographic studies of the prokaryotic KcsA potassium channel, for example, have shed much light on the structural basis of ion permeation through potassium channels and the mode of action of QAs.[12−17] Specifically, cocrystal structures of KcsA in complex with the symmetrical QA compound tetrabutylammonium (TBA) have demonstrated the precise location of the internal QA binding site, as well as the structural basis of the TBA−channel interaction (Figure 1B,C).[15−17] The TBA site is located in the internal water-filled cavity of the channel, directly underneath the innermost ion in the selectivity filter, and coincides with a dehydration transition site for permeant ions.[15] TBA binding is stabilized in the cavity

Received: April 30, 2014
Revised: August 1, 2014
Published: August 5, 2014

   dx.doi.org/10.1021/bi500525s | *Biochemistry* 2014, 53, 5365−5373

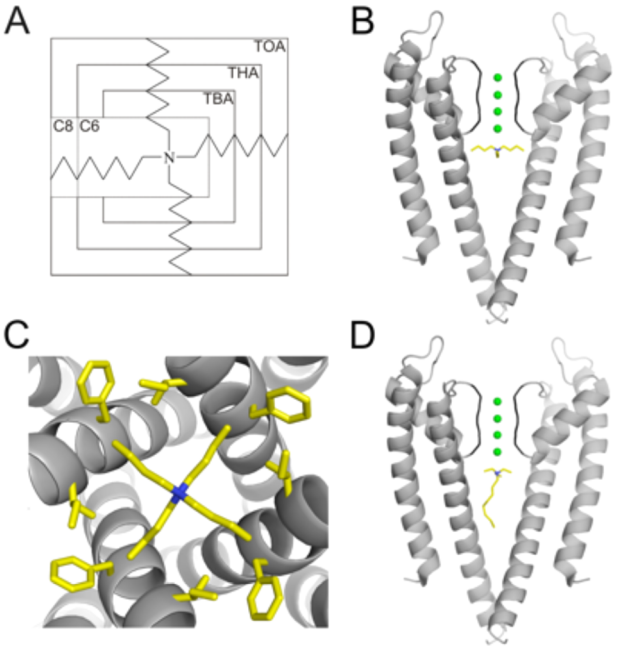

Figure 1. Blockade of potassium channels by quaternary ammonium compounds. (A) Structure of QA compounds. Tetrabutylammonium (TBA), tetrahexylammonium (THA), and tetraoctylammonium (TOA) are the symmetrical compounds used in this study. Triethylhexylammonium (C6) and triethyloctylammonium (C8) are asymmetrical long-chain QAs introduced by Armstrong.[3] (B) Overview of the KcsA potassium channel and the TBA binding site. Two diagonal subunits of the tetrameric channel are shown with the selectivity filter highlighted in black (residues 75−80). Potassium ions are shown as green spheres, and TBA is shown as sticks. The locations of the aqueous cavity and the inner gate are shown. (C) Detail of the TBA−channel interaction. View along the symmetry axis onto the TBA binding site. TBA and the side chains of I100 and F103 are highlighted. (D) Expected binding of C8. All structural figures were created using PyMOL.

through favorable van der Waals interactions between the alkyl chains of the blocker and the hydrophobic side chains of inner helix residues I100 and F103 (Figure 1C). This binding site and mechanism of blockade fit nicely with the precrystallographic concept of QA binding, a concept that can be extended to include more hydrophobic, longer-chain QA compounds (Figure 1D) if the long alkyl chains of the blockers are assumed to be stabilized by interactions with the predominantly hydrophobic lining of the ion pathway.[12]

In this study, we have cocrystallized KcsA with two symmetrical long-chain QA compounds expected to bind the internal QA binding site with high affinity:[18] tetrahexylammonium (THA) and tetraoctylammonium (TOA) (Figure 1A). We compare these two structures with the structure determined in the presence of TBA, a symmetrical intermediate-length QA. The three structures reveal the internal potassium channel binding site for long-chain, hydrophobic QA blockers. The internal receptor is unexpected in that it is located between the transmembrane helices of KcsA and consists of a hydrophobic binding pocket that allows direct communication between the aqueous cavity of the channel and the lipid bilayer, reminiscent of the fenestration observed in bacterial sodium channel structures.[19] Access to the pocket is apparently controlled by the rotameric state of residue F103, which is altered by binding of the long-chain blockers. Our structures also provide insight into the structural basis of closed-state blockade, use dependence of blockade, and drug trapping.

EXPERIMENTAL PROCEDURES

Protein Expression and Purification. KcsA was overexpressed and purified as described previously.[14] Briefly, the KcsA-L90C gene in pQE60 (Qiagen) was transformed into Novablue (Novagen) cells, and the cells were grown to logarithmic phase in Luria broth, induced with IPTG, and cultured. After cell membranes were disrupted by sonication, KcsA was solubilized with decyl maltoside (DM) and purified on a cobalt affinity column (Talon, Clontech). Thirty-five residues of KcsA were removed with chymotrypsin, and the truncated channel was further purified by gel filtration on a Superdex 200 column (GE Healthcare). The Fab fragment was obtained and purified as described previously.[14] Briefly, mouse hybridoma cells, generously provided by R. MacKinnon, were grown in cell culture, and the supernatant was harvested. The antibody was purified with protein A chromatography (GE Healthcare). The Fab fragment was obtained by papain proteolysis, followed by anion-exchange chromatography on Source Q and gel filtration on Superdex 200 (both GE Healthcare). The Fab−KcsA complex was formed overnight in a solution containing 150 mM KCl, 50 mM Tris, and 5 mM DM (pH 7.5). The complex was purified by gel filtration in a buffer containing 150 mM KNO_3, 50 mM HEPES, and 5 mM DM (pH 7.5).

Crystallization. TBA nitrate (5 mM) or THA or TOA nitrate (100 μM) was added to the dialyzed Fab−KcsA complex and the mixture incubated overnight. The complex was concentrated to ∼5 mg/mL, and crystals of space group *I*4 were grown at room temperature using the sitting drop vapor diffusion method as described previously.[14] Crystallization trials were set up using equal volumes of protein and reservoir solution [20−25% PEG 400, 50 mM magnesium acetate, and 50 mM sodium acetate (pH 5−5.6)].

Data Collection and Processing. Crystals were cryoprotected by incrementally increasing the precipitant concentration as described previously,[14] harvested in nylon loops, and immediately flash-cooled in liquid nitrogen. Data were measured under a stream of nitrogen at the GM/CA 22ID-B beamline at the Advanced Photon Source (APS) at Argonne National Laboratory (Argonne, IL). All data were integrated and scaled using XDS.[20] Phases were obtained by molecular replacement using PHASER[21] with the structure of the Fab−KcsA complex [Protein Data Bank (PDB) entry 1K4C] as the search model. The models were refined by several cycles of manual rebuilding with COOT,[22] followed by refinement using REFMAC.[23] Data collection and refinement statistics are listed in Table 1.

Functional Assay. Functional assays using ANTS fluorescence were performed as described previously.[24,25] Briefly, 1-palmitoyl-2-oleoyl-*sn*-glycero-3-phosphocholine (POPC) and 1-palmitoyl-2-oleoyl-*sn*-glycero-3-[phospho-*rac*-(1-glycerol)] (POPG) (Avanti Polar) at a ratio of 4:1 were solubilized in a buffer containing 100 mM KNO_3, 10 mM HEPES (pH 7.0), 10 mM succinic acid, 25 mM 8-aminonaphthalene-1,3,6-trisulfonic acid (ANTS), and 35 mM CHAPS. Purified KcsA was added at a lipid:protein molar ratio of ∼9000:1, and the detergent was removed with BioBeads SM-2 (Bio-Rad). The liposomes were extruded through a 100 nm polycarbonate filter, and extravesicular ANTS was removed by gel filtration on a PD-10 column (GE Healthcare) with 140 mM KNO_3, 10 mM

dx.doi.org/10.1021/bi500525s | *Biochemistry* 2014, 53, 5365−5373

Table 1. Data Collection and Refinement Statistics

	TBA	THA	TOA
wavelength (Å)	0.977	0.978	1.033
space group	*I*4	*I*4	*I*4
cell dimensions (Å)			
a	156.15	154.61	155.76
c	76.33	75.95	75.89
resolution (Å)	50.0−2.40 (2.54−2.40)	50.0−2.40 (2.54−2.40)	50.0−2.40 (2.54−2.40)
R_{sym} or R_{merge}	7.4 (44.1)	5.2 (58.3)	3.8 (48.4)
$I/\sigma I$	15.3 (3.5)	17.1 (2.1)	20.6 (2.5)
completeness (%)	99.5 (98.9)	98.1 (97.7)	97.8 (96.3)
redundancy	3.75 (3.75)	3.31 (3.31)	3.24 (3.27)
	Refinement		
resolution (Å)	30.0−2.40	30.0−2.40	30.0−2.40
no. of reflections	33912	32854	30907
R_{work}/R_{free}	20.2/24.9	19.2/24.8	20.0/24.1
no. of atoms	4422	4343	4378
protein	4130	4150	4096
ligand/ion	84	104	114
water	208	90	168
B factor (Å^2)			
protein	44.5	69.5	60.6
ligand	22.5	53.9	44.4
ions	31.0	39.1	42.4
lipid	58.6	74.2	69.7
water	45.8	58.8	61.1
root-mean-square deviation			
bond lengths (Å)	0.012	0.014	0.010
bond angles (deg)	1.336	1.310	1.260

HEPES (pH 7.0), and 10 mM succinic acid. The resulting KcsA:liposome ratio was ∼10:1. The QA compounds were dissolved in DMSO and added to the vesicle solution. The ANTS fluorescence was measured using a stopped-flow spectrofluorometer (SLM, Olis) by mixing the vesicle solution in single-mixing mode with an equal volume of quench buffer consisting of 50 mM $TlNO_3$, 94 mM KNO_3, 10 mM HEPES, and 10 mM succinic acid. The pH of the quench buffer was adjusted to obtain the described pH values in the mixing chamber. About 60 repeats were signal averaged and normalized. The time course of the fluorescence signal was fit to a stretched exponential, and the initial rate was determined at 10 ms as described previously.[25]

RESULTS

KcsA's Hydrophobic Binding Pocket: The Binding Site for Long-Chain QAs. To determine the location of the internal, hydrophobic QA binding site, the KcsA potassium channel was cocrystallized with tetrahexylammonium (THA) and tetraoctylammonium (TOA), two symmetrical analogues of the long-chain TEA derivatives originally used by Armstrong,[3] as well as with TBA, a symmetrical intermediate-length TEA analogue (Figure 1A). The TBA structure serves as a reference in these experiments and has previously been described.[15−17] All three compounds have 2-fold symmetry and are therefore more easily resolved in electron density maps of a 4-fold symmetrical channel than the better-studied, but nonsymmetrical, alkyl-triethylammonium compounds (Figure 1A). Indeed, we have determined structures of KcsA in complex with these compounds (C6, C8, and C10) at high resolution, but the symmetry mismatch leads to weak electron density of the bound QA alkyl chains (data not shown). All crystals were grown as KcsA−Fab complexes to improve diffraction, and in the presence of potassium as the permeant ion.[14] The cocrystals diffracted X-rays to ∼2.4 Å Bragg spacings at the synchrotron, and the structures were determined by molecular replacement using the KcsA−Fab complex in potassium (PDB entry 1K4C) as the search model (Table 1).

There are several consistent features among the structures (Figure 2). First, the ammonium headgroup of the three blockers binds at the same location in the cavity below the selectivity filter. Second, the three blockers all bind with the same quasi-planar symmetry (D_{2D}) that was first observed for TEA in the structure of carbamoyl phosphate synthetase,[26] allowing their four alkyl chains to extend laterally into the space between KcsA monomers (Figure 2A). Third, the orientation of the alkyl chains with respect to the symmetry axis is essentially the same for all three blockers; i.e., larger blockers recapitulate and extend the structural interactions of shorter blockers (Figure 2A). There is, however, a significant difference in the cavity at residue F103 between the TBA structure and the other two structures (Figure 2B). The side chain of F103 has adopted a new rotamer in the THA and TOA structures and now projects into the cavity, making room for the alkyl chains of the ligand to bind in the space previously occupied by the original rotamer. Although the rotation of a single bond may appear to be a subtle structural change, it has substantial implications here. The side chain of F103 in its original (TBA) rotamer is all that physically shields the aqueous cavity of the channel from the surrounding lipid bilayer. This can be illustrated with space-filling models of the three structures (Figure 2C). The side-chain rotation of F103 opens a lateral window in the channel between the internal cavity and the outside environment. There are thus three pathways into the

dx.doi.org/10.1021/bi500525s | *Biochemistry* 2014, 53, 5365−5373

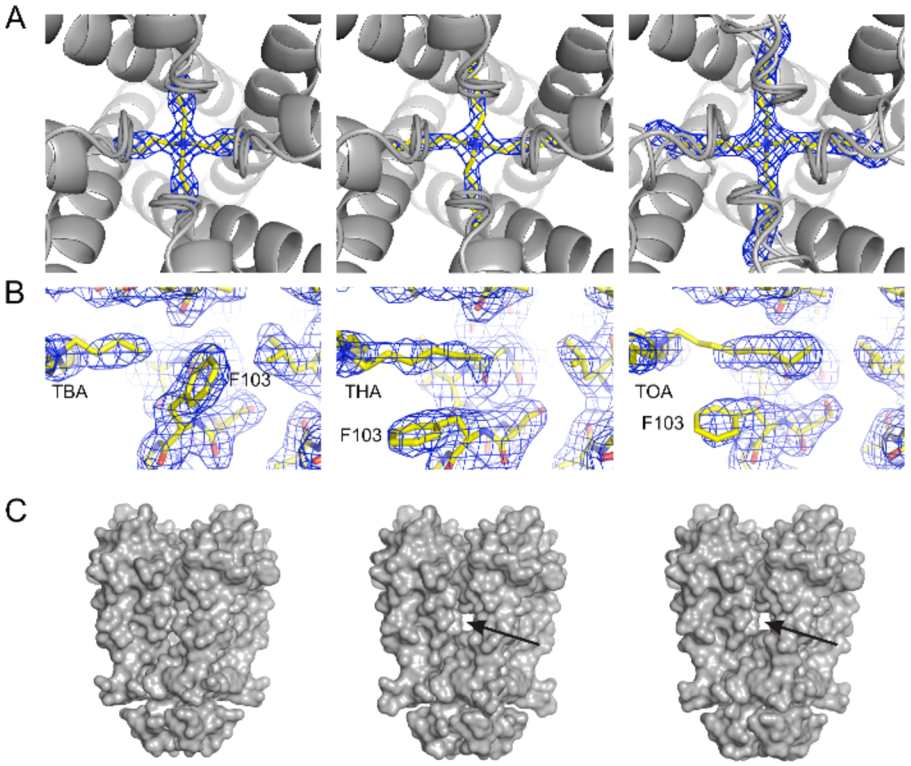

Figure 2. Hydrophobic binding site in KcsA. Comparison of the TBA (left), THA (middle), and TOA (right) structures. (A) View down the symmetry axis onto the QA binding site. KcsA is shown as gray ribbons, and the ligands are shown as sticks. The blue $2F_o - F_c$ maps are contoured at 1σ. (B) Side view at the height of the ligand. The $2F_o - F_c$ maps over the protein are contoured at 1.5σ, while $F_o - F_c$ omit maps (the ligand was omitted during map calculation) over the ligand are contoured at 3σ (2.5σ for THA). Note the F103 rotamer change between the TBA and the THA and TOA structures. (C) Outside view of the channel. The van der Waals surface of the channel is drawn using a 1.6 Å sphere. Note the lateral window in the THA and TOA structures (arrows).

central cavity of KcsA in the THA- and TOA-bound structures. Two of these pathways are the well-known aqueous access routes used by potassium ions along the symmetry axis of the channel. The third pathway connects the cavity laterally with the middle of the membrane.

Stabilization of Long-Chain QAs in the Hydrophobic Binding Pocket. Figure 3 demonstrates the incremental extension of alkyl chains into the hydrophobic pocket. The hexyl chain of THA initially recapitulates the butyl chain of TBA (Figure 3A) and can therefore maintain many of the van der Waals interactions known to stabilize TBA binding in the cavity (mainly to the side chains of the inner helix residues I100 and, in a new rotamer, F103). The peripheral ethylene of the hexyl chain undergoes additional van der Waals interactions with the main chain of the inner helix residues G99, the side chain of I100 from a neighboring subunit, and the main chain of T74 (Figure 3B). The octyl chain of TOA in turn recapitulates the interactions with the channel observed with TBA and THA and forms additional interactions with the peripheral ethylene (Figure 3C). These additional interactions occur with Cα of G99, the side chain of S102 (in a new rotamer compared to the THA-bound structure), the side chain of T74, and the side chain of outer helix residue L36.

Three findings involving the channel−blocker interaction are particularly noteworthy. First, the octyl chain of TOA is found to be in van der Waals contact with a residue of the outer helix. This interaction demonstrates that drug binding is not confined to the inner helix but that outer helix residues can participate if the ligand is able to penetrate deeply into the pocket. Second, both the hexyl and the octyl chains interact closely with the main chain of the inner helix at G99, a site thought to act as a pivot point or hinge in the gating of the channel.[27,28] This interaction is interesting in light of the observed drug trapping and gating effects of QA binding that were previously thought to occur inside the cavity and near the bundle crossing of the inner helices (Figure 1D).[12] Third, both long alkyl chains interact closely with the pore helix. The structural consequences of this interaction will be described next.

Ligand-Induced Conformational Changes in the Selectivity Filter. Figure 4 compares the state of the selectivity filter in the presence of TBA (short alkyl chain) and TOA (long alkyl chain). All crystals in this study were grown in the presence of the same potassium concentration (150 mM), were of similar quality, and were treated identically throughout all procedures (Table 1). In the presence of TBA, the selectivity filter adopts the same open and conductive conformation observed in its absence (Figure 4A, left).[16,17] In other words, binding of TBA does not alter the state of the selectivity filter with potassium as the permeant ion species. (It has previously been shown that TBA can alter the structure of the selectivity filter in the presence of thallium in what appears to be a thallium concentration-dependent manner.[15,16]) The open conformation of the selectivity filter is characterized by the presence of four, approximately equally occupied, potassium binding sites (Figure 4B, left) and is accompanied by a hydrogen bond network that includes a set of specific interactions among residues W68, E71, and D80 that maintain the structural integrity of the filter in the conducting state.[14,29,30] In the presence of TOA, however, the selectivity filter adopts the collapsed conformation observed at low

dx.doi.org/10.1021/bi500525s | *Biochemistry* 2014, 53, 5365−5373

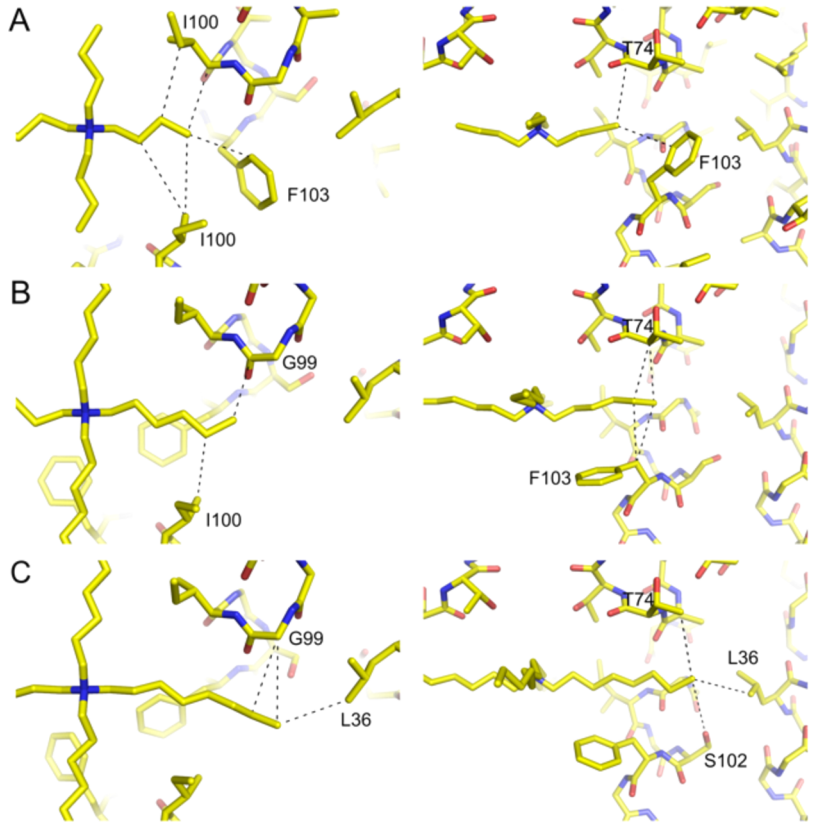

Figure 3. Incremental extension of QAs into the hydrophobic binding pocket. Views along the symmetry axis (left) and side views at the height of the hydrophobic pocket (right) are shown. In each panel, only the van der Waals interactions not previously observed with shorter QAs are shown. (A) Interaction between the C4 alkyl chain of TBA and residues I100 and F103. Favorable van der Waals interactions are shown. (B) Favorable interactions between the peripheral ethylene of the C6 alkyl chain of THA and T74, G99, I100, and F103 are shown. (C) Favorable interactions between the peripheral ethylene of the C8 alkyl chain of TOA and L36, T74, G99, and S102 are shown.

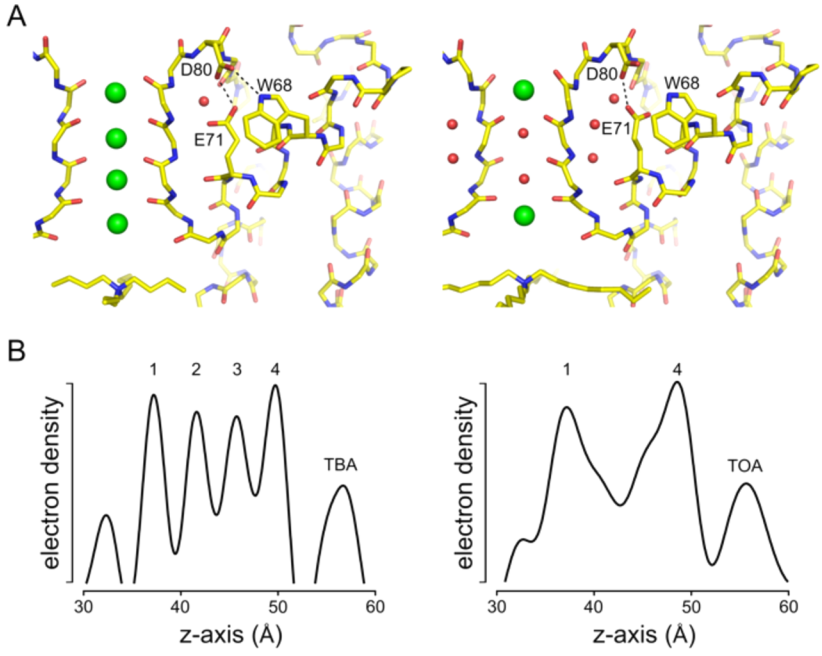

Figure 4. Structural change in the selectivity filter induced by long-chain QA binding. Comparison of the TBA (left) and TOA (right) structures. (A) Side view of the selectivity filter. The main chain of the selectivity filter as well as the side chains of residues W68, E71, and D80 are shown as sticks. Potassium ions are illustrated as green spheres, water molecules as red spheres, and important stabilizing hydrogen bonds as black dotted lines. (B) Normalized one-dimensional electron density along the symmetry axis. The ion numbering is from outside to inside. The map was calculated using MAPMAN,[47] and the selectivity filter and ions were omitted during $F_o - F_c$ map calculation.

dx.doi.org/10.1021/bi500525s | *Biochemistry* 2014, 53, 5365−5373

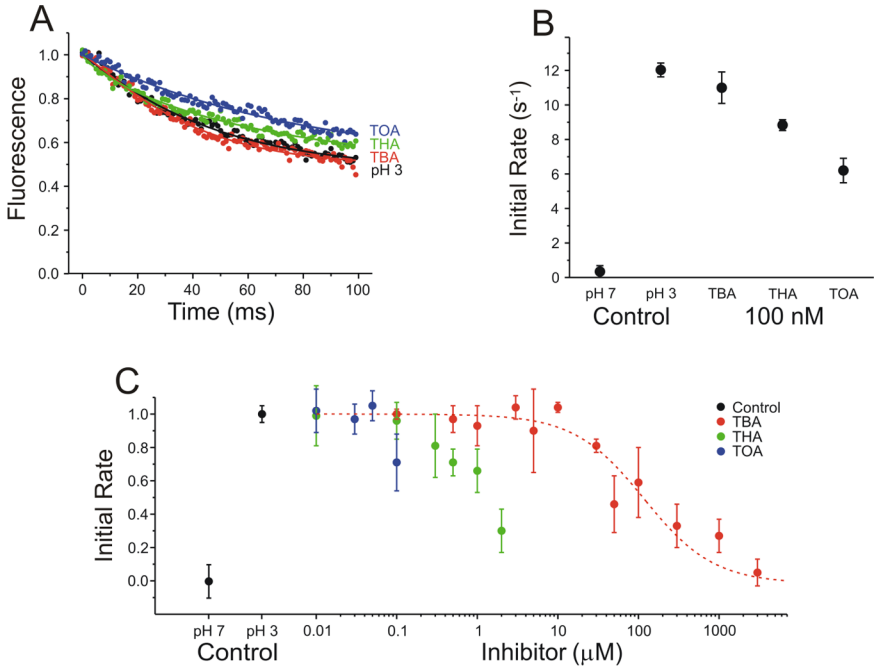

Figure 5. Functional assay that shows an incremental increase in QA binding affinity with increasing alkyl-chain length. (A) Fluorescence traces of ANTS-loaded vesicles containing reconstituted KcsA mixed with thallium nitrate at pH 3. The low pH transiently opens KcsA and allows extravesicular thallium to enter the vesicles and quench ANTS fluorescence. The stopped-flow experiment was performed in the absence (pH 3, black) and presence of 100 nM TBA (red), THA (green), or TOA (blue) in the vesicle solution. (B) The averages and standard deviations (n = 4) of the fluorescence decay rate measured at 10 ms are shown for five conditions. The control conditions demonstrate the rate of closed (pH 7) and open (pH 3) channels in the absence of QA compounds. The 100 nM conditions show the different rates in the presence of a constant concentration of the three QA compounds. (C) Dose–response curves of the three QA compounds. The averages and standard deviations (n = 3–14) of the initial rates normalized to the closed (pH 7) and open (pH 3) conditions (control) are shown. The red dotted line is a fit of the TBA data to the Hill equation with an inhibition constant of 119 μM and a Hill coefficient of 1. The solubility limit in the assay buffer is ~100 nM for TOA and ~2 μM for THA.

potassium concentrations.[14,31] (The selectivity filter adopts a very similar conformation in the presence of THA, but evidence of external THA binding, as observed by weak electron density for the ligand at the external TEA site, complicates the analysis in this case.) The collapsed conformation of the selectivity filter is thought to be nonconductive[14,32−34] and is characterized by the presence of only two potassium ions (Figure 4B, right), an altered hydrogen bond network, and the binding of three water molecules[14,29,35] (Figure 4A, right). Unlike TBA, TOA is thus capable of shifting the conformational state of the selectivity filter under otherwise identical conditions.

Increasing Affinity with Increasing Alkyl-Chain Length. Figure 5 shows results from a functional assay to determine the relative binding energies of the interaction of KcsA with the three QA compounds. In this stopped-flow assay, vesicles containing KcsA and loaded with the fluorescent dye ANTS are mixed with a low-pH solution containing thallium. The low pH activates KcsA and allows thallium to enter the vesicles through open KcsA channels and quench ANTS fluorescence. The number of open channels is approximately proportional to the initial decay of the fluorescence trace.[25] Figure 5A shows the fluorescence trace for control vesicles (pH 3) and vesicles containing a constant concentration of 100 nM of each compound. The control and TBA traces decay almost identically, indicating that very few channels are blocked by 100 nM TBA. The decay is notably slower in the presence of 100 nM THA (Figure 5B), indicating that more channels are blocked in the presence of the same concentration of THA. The decay is even slower in the presence of 100 nM TOA (Figure 5B). The low solubility of THA and TOA and the adverse effect of DMSO limit the assay to concentrations of 100 nM (TOA) and 2 μM (THA), respectively. Figure 5C shows dose–response curves of the three inhibitors up to their solubility limit in the assay buffer. The observed inhibition constant of TBA is ~120 μM. While the obtainable data are insufficient to determine the inhibition constants for THA and TOA with acceptable accuracy, they are sufficient to demonstrate the basic concept of increasing binding affinity with increasing alkyl-chain length, consistent with the observed incremental increase in the number of van der Waals interactions in the three structures.

DISCUSSION

Hydrophobic Drug Binding in Potassium and Sodium Channels. The cocrystal structures of KcsA with THA and TOA demonstrate the internal hydrophobic binding site for long-chain QA compounds in the KcsA potassium channel (Figure 2A). The configuration of this binding site is unexpected. The alkyl chains of the blockers are not accommodated in the central cavity of the channel as anticipated but instead bind within a hydrophobic binding pocket, a space lined by predominantly hydrophobic moieties from two adjacent inner helices and a pore helix. The alkyl chains gain access to the pocket from the central cavity through rotation of the phenylalanine side chain at position 103. The most striking consequence of this rotameric adjustment of the channel to drug binding is the opening of a direct lateral conduit between the internal cavity and the lipid bilayer, a third

dx.doi.org/10.1021/bi500525s | Biochemistry 2014, 53, 5365−5373

pathway into the central cavity of the channel (Figure 2C). Given the high degree of structural conservation among the pore-forming units of cation selective channels,[36,37] it appears likely that the hydrophobic binding pocket represents a conserved hydrophobic binding site in potassium and related ion channels. Indeed, a similar hydrophobic access pathway has been observed in sodium channel structures.[19,38] The corresponding pocket has been proposed to constitute the tetracaine binding site in voltage-dependent sodium channels.[39]

Stabilization of the Nonconducting State by QAs. It has been shown that the equilibrium between the open and collapsed states of KcsA's selectivity filter can be influenced by the permeant ion species, the binding of an antibody fragment used to obtain high-resolution crystals, mutations in or near the selectivity filter, the gating state of the channel, and the binding of QA compounds to either side of the membrane.[14,15,29,30,32,33,40,41] The data presented here demonstrate that the collapsed conformation is also induced by QA compounds in the continued presence of high concentrations of potassium. The differences between the TBA and TOA structures suggest that this occurs because of an interaction between the octyl chain of TOA and the pore helix: placing the TOA ligand into the TBA structure (with TBA and the F103 side chain removed) leads to a prominent steric clash between the alkyl chains of TOA and pore residues T74 and T75 (data not shown). It thus appears that the alkyl chain pushes the pore helix upward and forces the selectivity filter into a nonconducting state. Alternatively stated, the binding pocket is accessible to the octyl chain only in the nonconducting state of the channel. It could be argued, therefore, that long-chain QAs inhibit potassium channels through two different mechanisms, namely, physical occlusion and allosteric regulation, and that these two mechanisms manifest themselves functionally as open channel block and promotion of slow inactivation, respectively. It follows that it may be possible to block permeation without physically occluding the permeation pathway simply by stabilizing the nonconducting state of the selectivity filter. Such a mechanism would be expected to show a high degree of cooperativity if the blocker were completely excluded from the symmetry axis. There is evidence suggesting that this mechanism may indeed be operational: disubstituted cyclohexyl compounds inhibit the Kv1.3 potassium channel with an apparent stoichiometry of 2:1 and may access their binding sites through a hydrophobic pathway.[42,43]

KcsA as a Model for QA Binding in Kv-Type Potassium Channels. Most of the functional data describing QA blockade of potassium channels have been obtained on voltage-gated (Kv-type) channels.[2−11,18] Figure 6 demonstrates the structural conservation between KcsA and the pore domain of the eukaryotic Kv1.2 channel.[44,45] A high degree of structural conservation is maintained at the QA binding site despite differences in the gating mechanics (a glycine residue acting as a hinge in KcsA, a PNP motif in Kv1.2) and gating states (KcsA is closed; Kv1.2 is open) of the two channels. The residues colored red contribute to the TOA binding site in KcsA and are similarly situated in the Kv1.2 structure. The most notable structural differences are located below the glycine hinge at KcsA positions S102 and F103 (T401 and I402 in Kv1.2, respectively) and are thus likely due, at least in part, to the different gating states of the two channels. The side chains of the remaining inner helix residues involved in TOA binding (A73, T74, T75, G99, and I100) are chemically very similar to their corresponding Kv1.2 residues (M372, T373, T374, G398, and V399). The KcsA binding site may thus provide sufficient structural conservation to provide useful insight into the QA binding site in Kv-type potassium channels.

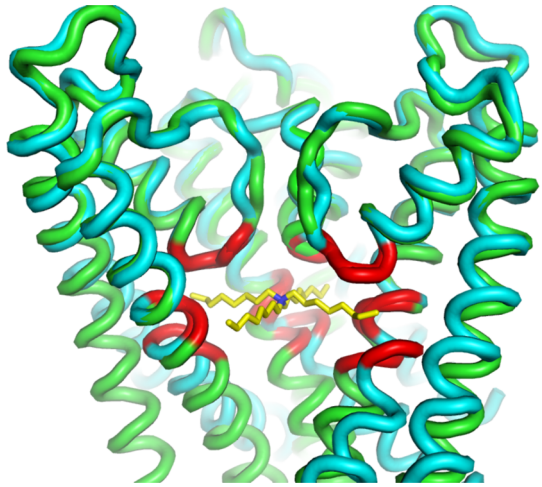

Figure 6. Structural conservation of the QA binding site. Structural alignment of the pore regions of KcsA (TOA structure) and Kv1.2 (PDB entry 2A79) generated by aligning KcsA residues L40−G99 with Kv1.2 residues V339−G398. Three monomers of each channel are shown; KcsA is colored green and Kv1.2 cyan. TOA is shown as sticks. Residues of KcsA within van der Waals distance of bound TOA and their Kv1.2 counterparts are colored red: A73 (M372), T74 (T373), T75 (T374), G99 (G398), I100 (V399), S102 (T401), and F103 (I402).

Mechanism of Long-Chain QA Stabilization. Armstrong's landmark experiments on the squid giant axon demonstrated that the hydrophobicity of a QA blocker is a major determinant of its ability to block potassium channels.[3] Using mutagenesis studies, Yellen and co-workers found that increasing the hydrophobic character of the amino acid at position 469 in Shaker (corresponding to S102 in KcsA and T401 in Kv1.2) increased the affinity of the blockers by at least 1 order of magnitude. In contrast, a mutation known to drastically decrease the affinity of TEA itself had little effect on the affinity of long-chain QA blockers.[2,6] These and related findings were explained by proposing two competing binding sites for long-chain QAs: a hydrophilic headgroup binding site (corresponding to the internal TEA site) and a hydrophobic tail binding site.[7] The present structures support this hypothesis and locate the headgroup binding site in the aqueous cavity and the tail binding site in the hydrophobic binding pocket. The hallmark result observed in eukaryotic channels of increasing binding affinity with increasing alkyl-chain length of the QA compound was also observed in KcsA (Figure 5C), further substantiating the general applicability of the binding mechanism described here.

Mechanism of Drug Trapping and Long-Chain QA Effects on Gating. Given the closed state of the internal activation gate [inner helix bundle (Figure 1B)] and the presence of bound drug in the cavity, it would seem that the structures described here capture the channel in a trapped state. Trapping is important pharmacologically as the ability to bind the channel in the closed state potentiates the actions of drugs and underlies use dependence, the accumulation of inhibition with repetitive stimuli.[9] The Yellen laboratory has demonstrated that modifications at a single amino acid position can switch the Shaker channel from a nontrapping mode to a

dx.doi.org/10.1021/bi500525s | Biochemistry 2014, 53, 5365−5373

trapping mode (I470A and I470C).[9,10] Because the mutations that facilitated trapping in their experiments reduced the volume of a side chain thought to line the cavity, the results were interpreted in terms of cavity size.[9] The crystallographic data reported here suggest a slightly different mechanism. Instead, the long-chain QA trapping properties, or lack thereof, of the Shaker channel might be due to the energetic cost of accessing the pocket, i.e., the low probability of the I470 side chain to change rotamer and move from the hydrophobic pocket to the more hydrophilic cavity environment.

The phrase "foot in the door" is frequently used to describe the blocking mechanism of QAs in potassium channels. It implies that these blockers impose themselves between the moving parts of the gating machinery of the channel. The general location of the hydrophobic binding site described here and the interaction between the alkyl chains of the blockers and the inner helix main chain at residue G99 (Figure 3) suggest that an alternative phrase such as "finger in the hinge" might more aptly describe the action of these blockers. The interference does not occur, at least in KcsA, near the activation gate of the channel at the bundle crossing of the inner helices, but near residues G99 and F103. While the amplitude of the gating transition may be larger elsewhere, these two residues are strategically located at or near the hinge of the gating movement where small but critical structural rearrangements take place. By interacting with this mechanically central part of the channel, QAs and other drugs may be able to influence the relative stability of the different gating states with functional consequences that can vary from subtle shifts in the gating equilibrium[9,46] to the more dramatic phenomena observed by Armstrong.[3]

■ ASSOCIATED CONTENT

Accession Codes

The coordinates and structure factors of the Fab−KcsA complex with TBA, THA, and TOA have been deposited as Protein Data Bank entries 2JK5, 4UUJ, and 2W0F, respectively.

■ AUTHOR INFORMATION

Corresponding Author

*Rosalind Franklin University, 3333 Green Bay Rd., North Chicago, IL 60064. E-mail: adrian.gross@rosalindfranklin.edu. Telephone: (847) 578-8507. Fax: (847) 578-3240.

Funding

This work was supported by National Institutes of Health Grant GM58568 to A.G. Support from the R. H. Lurie Comprehensive Cancer Center of Northwestern University to the Structural Biology Facility is acknowledged.

Notes

The authors declare no competing financial interest.

■ ACKNOWLEDGMENTS

We thank I. Popova for antibody production and M. Becker for assistance with data collection. Portions of this work were conducted at LS-CAT. Use of the APS is supported by the U.S. Department of Energy (Contract W-31-109-Eng-38).

■ ABBREVIATIONS

ANTS, 8-aminonaphthalene-1,3,6-trisulfonic acid; APS, Advanced Photon Source; CHAPS, 3-[(3-cholamidopropyl)-dimethylammonio]-1-propanesulfonate; C4, butyltriethylammonium; C6, hexyltriethylammonium; C8, octyltriethylammonium; C10, decyltriethylammonium; DM, decyl maltoside; DMSO, dimethyl sulfoxide; Fab, fragment antigen binding; HEPES, 4-(2-hydroxyethyl)-1-piperazineethanesulfonic acid; IPTG, isopropyl β-D-1-thiogalactopyranoside; KCl, potassium chloride; KNO_3, potassium nitrate; PEG, polyethylene glycol; POPC, 1-palmitoyl-2-oleoyl-*sn*-glycero-3-phosphocholine; POPG, 1-palmitoyl-2-oleoyl-*sn*-glycero-3-[phospho-*rac*-1-glycerol]; TBA, tetrabutylammonium; TEA, tetraethylammonium; THA, tetrahexylammonium; $TlNO_3$, thallium nitrate; TOA, tetraoctylammonium; Tris, tris(hydroxymethyl)aminomethane; QA, quaternary ammonium.

■ REFERENCES

(1) Hille, B. (1967) The selective inhibition of delayed potassium currents in nerve by tetraethylammonium ion. *J. Gen. Physiol. 50*, 1287−1302.

(2) Yellen, G., Jurman, M. E., Abramson, T., and MacKinnon, R. (1991) Mutations affecting internal TEA blockade identify the probable pore-forming region of a K^+ channel. *Science 251*, 939−942.

(3) Armstrong, C. M. (1971) Interaction of tetraethylammonium ion derivatives with the potassium channels of giant axons. *J. Gen. Physiol. 58*, 413−437.

(4) Armstrong, C. M., and Binstock, L. (1965) Anomalous Rectification in the Squid Giant Axon Injected with Tetraethylammonium Chloride. *J. Gen. Physiol. 48*, 859−872.

(5) Armstrong, C. M. (1969) Inactivation of the potassium conductance and related phenomena caused by quaternary ammonium ion injection in squid axons. *J. Gen. Physiol. 54*, 553−575.

(6) Choi, K. L., Mossman, C., Aube, J., and Yellen, G. (1993) The internal quaternary ammonium receptor site of Shaker potassium channels. *Neuron 10*, 533−541.

(7) Baukrowitz, T., and Yellen, G. (1996) Two functionally distinct subsites for the binding of internal blockers to the pore of voltage-activated K^+ channels. *Proc. Natl. Acad. Sci. U.S.A. 93*, 13357−13361.

(8) Baukrowitz, T., and Yellen, G. (1996) Use-dependent blockers and exit rate of the last ion from the multi-ion pore of a K^+ channel. *Science 271*, 653−656.

(9) Holmgren, M., Smith, P. L., and Yellen, G. (1997) Trapping of organic blockers by closing of voltage-dependent K^+ channels: Evidence for a trap door mechanism of activation gating. *J. Gen. Physiol. 109*, 527−535.

(10) Melishchuk, A., and Armstrong, C. M. (2001) Mechanism underlying slow kinetics of the OFF gating current in Shaker potassium channel. *Biophys. J. 80*, 2167−2175.

(11) Armstrong, C. M., and Hille, B. (1972) The inner quaternary ammonium ion receptor in potassium channels of the node of Ranvier. *J. Gen. Physiol. 59*, 388−400.

(12) Doyle, D. A., Cabral, J. M., Pfuetzner, R. A., Kuo, A., Gulbis, J. M., Cohen, S. L., Chait, B. T., and MacKinnon, R. (1998) The structure of the potassium channel: Molecular basis of K^+ conduction and selectivity. *Science 280*, 69−77.

(13) Zhou, M., Morais-Cabral, J. H., Mann, S., and MacKinnon, R. (2001) Potassium channel receptor site for the inactivation gate and quaternary amine inhibitors. *Nature 411*, 657−661.

(14) Zhou, Y., Morais-Cabral, J. H., Kaufman, A., and MacKinnon, R. (2001) Chemistry of ion coordination and hydration revealed by a K^+ channel-Fab complex at 2.0 Å resolution. *Nature 414*, 43−48.

(15) Lenaeus, M. J., Vamvouka, M., Focia, P. J., and Gross, A. (2005) Structural basis of TEA blockade in a model potassium channel. *Nat. Struct. Mol. Biol. 12*, 454−459.

(16) Yohannan, S., Hu, Y., and Zhou, Y. (2007) Crystallographic study of the tetrabutylammonium block to the KcsA K^+ channel. *J. Mol. Biol. 366*, 806−814.

(17) Faraldo-Gomez, J. D., Kutluay, E., Jogini, V., Zhao, Y., Heginbotham, L., and Roux, B. (2007) Mechanism of intracellular block of the KcsA K^+ channel by tetrabutylammonium: Insights from X-ray crystallography, electrophysiology and replica-exchange molecular dynamics simulations. *J. Mol. Biol. 365*, 649−662.

(18) French, R. J., and Shoukimas, J. J. (1981) Blockage of squid axon potassium conductance by internal tetra-N-alkylammonium ions of various sizes. *Biophys. J. 34*, 271−291.
(19) Payandeh, J., Scheuer, T., Zheng, N., and Catterall, W. A. (2011) The crystal structure of a voltage-gated sodium channel. *Nature 475*, 353−358.
(20) Kabsch, W. (1993) Automatic processing of rotation diffraction data from crystals of initially unknown symmetry and cell constants. *J. Appl. Crystallogr. 26*, 795−800.
(21) McCoy, A. J., Grosse-Kunstleve, R. W., Adams, P. D., Winn, M. D., Storoni, L. C., and Read, R. J. (2007) Phaser crystallographic software. *J. Appl. Crystallogr. 40*, 658−674.
(22) Emsley, P., and Cowtan, K. (2004) Coot: Model-building tools for molecular graphics. *Acta Crystallogr. D60*, 2126−2132.
(23) Murshudov, G. N., Vagin, A. A., and Dodson, E. J. (1997) Refinement of macromolecular structures by the maximum-likelihood method. *Acta Crystallogr. D53*, 240−255.
(24) Ingolfsson, H. I., and Andersen, O. S. (2010) Screening for small molecules' bilayer-modifying potential using a gramicidin-based fluorescence assay. *Assay Drug Dev. Technol. 8*, 427−436.
(25) Rusinova, R., Kim, D. M., Nimigean, C. M., and Andersen, O. S. (2014) Regulation of ion channel function by the host lipid bilayer examined by a stopped-flow spectrofluorometric assay. *Biophys. J. 106*, 1070−1078.
(26) Thoden, J. B., Miran, S. G., Phillips, J. C., Howard, A. J., Raushel, F. M., and Holden, H. M. (1998) Carbamoyl phosphate synthetase: Caught in the act of glutamine hydrolysis. *Biochemistry 37*, 8825−8831.
(27) Jiang, Y., Lee, A., Chen, J., Cadene, M., Chait, B. T., and MacKinnon, R. (2002) Crystal structure and mechanism of a calcium-gated potassium channel. *Nature 417*, 515−522.
(28) Jiang, Y., Lee, A., Chen, J., Cadene, M., Chait, B. T., and MacKinnon, R. (2002) The open pore conformation of potassium channels. *Nature 417*, 523−526.
(29) Cordero-Morales, J. F., Cuello, L. G., Zhao, Y., Jogini, V., Cortes, D. M., Roux, B., and Perozo, E. (2006) Molecular determinants of gating at the potassium-channel selectivity filter. *Nat. Struct. Mol. Biol. 13*, 311−318.
(30) Cordero-Morales, J. F., Jogini, V., Lewis, A., Vasquez, V., Cortes, D. M., Roux, B., and Perozo, E. (2007) Molecular driving forces determining potassium channel slow inactivation. *Nat. Struct. Mol. Biol. 14*, 1062−1069.
(31) Zhou, Y., and MacKinnon, R. (2003) The occupancy of ions in the K^+ selectivity filter: Charge balance and coupling of ion binding to a protein conformational change underlie high conduction rates. *J. Mol. Biol. 333*, 965−975.
(32) Lockless, S. W., Zhou, M., and MacKinnon, R. (2007) Structural and thermodynamic properties of selective ion binding in a K^+ channel. *PLoS Biol. 5*, e121.
(33) Cuello, L. G., Jogini, V., Cortes, D. M., and Perozo, E. (2010) Structural mechanism of C-type inactivation in K^+ channels. *Nature 466*, 203−208.
(34) Cuello, L. G., Jogini, V., Cortes, D. M., Pan, A. C., Gagnon, D. G., Dalmas, O., Cordero-Morales, J. F., Chakrapani, S., Roux, B., and Perozo, E. (2010) Structural basis for the coupling between activation and inactivation gates in K^+ channels. *Nature 466*, 272−275.
(35) Ostmeyer, J., Chakrapani, S., Pan, A. C., Perozo, E., and Roux, B. (2013) Recovery from slow inactivation in K^+ channels is controlled by water molecules. *Nature 501*, 121−124.
(36) Lu, Z., Klem, A. M., and Ramu, Y. (2001) Ion conduction pore is conserved among potassium channels. *Nature 413*, 809−813.
(37) Shealy, R. T., Murphy, A. D., Ramarathnam, R., Jakobsson, E., and Subramaniam, S. (2003) Sequence-function analysis of the K^+-selective family of ion channels using a comprehensive alignment and the KcsA channel structure. *Biophys. J. 84*, 2929−2942.
(38) Payandeh, J., Gamal El-Din, T. M., Scheuer, T., Zheng, N., and Catterall, W. A. (2012) Crystal structure of a voltage-gated sodium channel in two potentially inactivated states. *Nature 486*, 135−139.
(39) Bruhova, I., Tikhonov, D. B., and Zhorov, B. S. (2008) Access and binding of local anesthetics in the closed sodium channel. *Mol. Pharmacol. 74*, 1033−1045.
(40) Zhou, M., and MacKinnon, R. (2004) A mutant KcsA K^+ channel with altered conduction properties and selectivity filter ion distribution. *J. Mol. Biol. 338*, 839−846.
(41) Valiyaveetil, F. I., Leonetti, M., Muir, T. W., and Mackinnon, R. (2006) Ion selectivity in a semisynthetic K^+ channel locked in the conductive conformation. *Science 314*, 1004−1007.
(42) Schmalhofer, W. A., Bao, J., McManus, O. B., Green, B., Matyskiela, M., Wunderler, D., Bugianesi, R. M., Felix, J. P., Hanner, M., Linde-Arias, A. R., Ponte, C. G., Velasco, L., Koo, G., Staruch, M. J., Miao, S., Parsons, W. H., Rupprecht, K., Slaughter, R. S., Kaczorowski, G. J., and Garcia, M. L. (2002) Identification of a new class of inhibitors of the voltage-gated potassium channel, Kv1.3, with immunosuppressant properties. *Biochemistry 41*, 7781−7794.
(43) Schmalhofer, W. A., Slaughter, R. S., Matyskiela, M., Felix, J. P., Tang, Y. S., Rupprecht, K., Kaczorowski, G. J., and Garcia, M. L. (2003) Di-substituted cyclohexyl derivatives bind to two identical sites with positive cooperativity on the voltage-gated potassium channel, K(v)1.3. *Biochemistry 42*, 4733−4743.
(44) Long, S. B., Campbell, E. B., and MacKinnon, R. (2005) Crystal structure of a mammalian voltage-dependent Shaker family K^+ channel. *Science 309*, 897−903.
(45) Long, S. B., Tao, X., Campbell, E. B., and MacKinnon, R. (2007) Atomic structure of a voltage-dependent K^+ channel in a lipid membrane-like environment. *Nature 450*, 376−382.
(46) Contreras, J. E., and Holmgren, M. (2006) Access of quaternary ammonium blockers to the internal pore of cyclic nucleotide-gated channels: Implications for the location of the gate. *J. Gen. Physiol. 127*, 481−494.
(47) Kleywegt, G. J., and Jones, T. A. (1996) xdlMAPMAN and xdlDATAMAN: Programs for reformatting, analysis and manipulation of biomacromolecular electron-density maps and reflection data sets. *Acta Crystallogr. D52*, 826−828.